Laser cooling and imaging of individual radioactive $^{90}Sr^{+}$ ions

Kyunghun Jung,[1] Yoshihiro Iwata,[1] Masabumi Miyabe,[2] Kazuhiro Yamamoto,[3] Tomohisa Yonezu,[1] Ikuo Wakaida,[2] and Shuichi Hasegawa[1,3]

[1]*Nuclear Professional School, The University of Tokyo, 2-22 Shirane, Shirakata, Tokai, Naka, Ibaraki, 319-1188, Japan*

[2]*Remote Analytical Technology Group, Collaborative Laboratories for Advanced Decommissioning Sciences, Japan Atomic Energy Agency, 2-4 Shirane, Shirakata, Tokai-mura, Naka-gun, Ibaraki, 319-1195, Japan*

[3]*Department of Nuclear Engineering and Management, The University of Tokyo, 7-3-1 Hongo, Bunkyo-ku, Tokyo 113-8656, Japan*

(Received 4 August 2017; published 30 October 2017)

We have developed an apparatus integrating resonance-ionization, ion-trap, and laser-cooling techniques for an ultratrace radioactive isotope ^{90}Sr analysis. Trapped $^{90}Sr^{+}$ isotope ions were laser cooled, and their $4d\,^2D_{3/2} \rightarrow 5p\,^2P_{1/2}$ transition isotope shift was experimentally measured to be $-281(17)$ MHz by comparing individual spectra of $^{88}Sr^{+}$ and $^{90}Sr^{+}$ ions. Crystallization of $^{90}Sr^{+}$ was carried out using the resonance frequency value confirmed in our experiment, and then $^{90}Sr^{+}$ individual ions were successfully observed.

DOI: 10.1103/PhysRevA.96.043424

I. INTRODUCTION

One of the most notable radionuclides released from the Fukushima Daiichi nuclear power plant accident is the radioactive fission product ^{90}Sr, which decays by emitting a β ray of 0.546 MeV with a half-life of 28.8 years. Because this alkaline-earth atom has chemical properties similar to those of calcium, it is readily incorporated into the human body, and hence, the subsequent effects of internal radiation exposure give us reason to be concerned [1]. However direct measurement of the radiation is difficult due to the low energy of the β ray. Therefore, producing a radioactivity equilibrium with its daughter nuclide ^{90}Y after chemical separation is usually performed for its standard measurement [2]. However, the measurement procedure is extremely complicated and time-consuming. Hence, a method combining Sr resin and inductively coupled plasma–mass spectroscopy (ICP-MS) was recently developed for ^{90}Sr analysis. In this method, interfering isobars ^{90}Zr and ^{90}Y are first removed by resin adsorption, and the residuals are then chemically converted into oxides inside the ICP-MS for further reduction. Analysis of ^{90}Sr in the soil surface has been demonstrated using this method [3]. However, analysis is expected to be difficult with this technique if the sample contains a large amount of the other alkaline-earth elements or ^{88}Sr. Resonance ionization mass spectroscopy (RIMS) has been studied as an analytical method using lasers because it enables ionization of ^{90}Sr with high selectivity. Unfortunately, since the $\Delta\nu^{90-88}$ isotope shift overlaps with $\Delta\nu^{86-88}$ due to the characteristics of Sr nuclei, Bushaw and Cannon reported that the isotope selectivity obtained through the three-step ionization scheme is insufficient for the analysis [4].

Consequently, we have proposed an isotope-selective and highly sensitive analytical technique through the use of an ion trap. Because trapped ions cooled to a cryogenic temperature by lasers make it possible to study pure quantum systems [5], the ion-trap laser-cooling technique is actively used in fields such as quantum information processing [6], frequency standards [7], and high-precision spectroscopy for nuclear structure research [8]. Only the isotope of interest can be selectively cooled with this technique, making it possible to remove unwanted isotopes and isobars from the trap [9]. Therefore, the isotope selectivity of the apparatus can be improved if the mass-separated ions of interest are trapped by the rf field and then selectively laser cooled. When the kinetic energy of the ions was reduced by laser cooling, the relative position of the crystallized ions was determined. By counting the crystallized individual ions from the CCD camera image, the influence of background signals and isobars can be avoided during analysis. To demonstrate this background-free observation, we have developed an ion-trap apparatus that uses ICP-MS as an ion source [10,11].

However, an ion source with high isotope selectivity is required for ^{90}Sr analysis since ionization in the ICP-MS is indiscriminately performed by argon plasma. Therefore, we are developing an ion-trap device that adopts RIMS as an ion source. Our very first aim was trapping $^{90}Sr^{+}$ with the constructed device. To the best of our knowledge, $^{90}Sr^{+}$ laser cooling has not been realized so far, and no isotope-shift data $\Delta\nu^{90-88}$ have been published for the $4d\,^2D_{3/2} \rightarrow 5p\,^2P_{1/2}$ transition required for laser cooling as yet. Therefore, in this paper, $^{90}Sr^{+}$ ions generated by resonance ionization from a concentrated solution are trapped and laser cooled as fundamental research. The results of isotope-shift measurements of the $4d\,^2D_{3/2} \rightarrow 5p\,^2P_{1/2}$ transition are provided, and imaging of trapped individual $^{90}Sr^{+}$ ions is also reported.

II. EXPERIMENTAL SETUP

A. Apparatus and methods

A schematic diagram of our apparatus developed for the ion trap is shown in Fig. 1. This apparatus consists of three sections: an ion-source section, a mass-analysis section, and an ion-trap section.

In the ion-source section, neutral atoms generated from an atomic vapor source were ionized by resonance ionization. A Sr standard solution [12] was used as a stable isotope ion source for the experiment. This solution is provided in the form of $SrCl_2$. The solution was dropped on titanium foil and heated to induce a reduction reaction as expressed by the following equation for atomization:

$$2SrCl_2 + Ti \rightarrow 2Sr + TiCl_4. \quad (1)$$

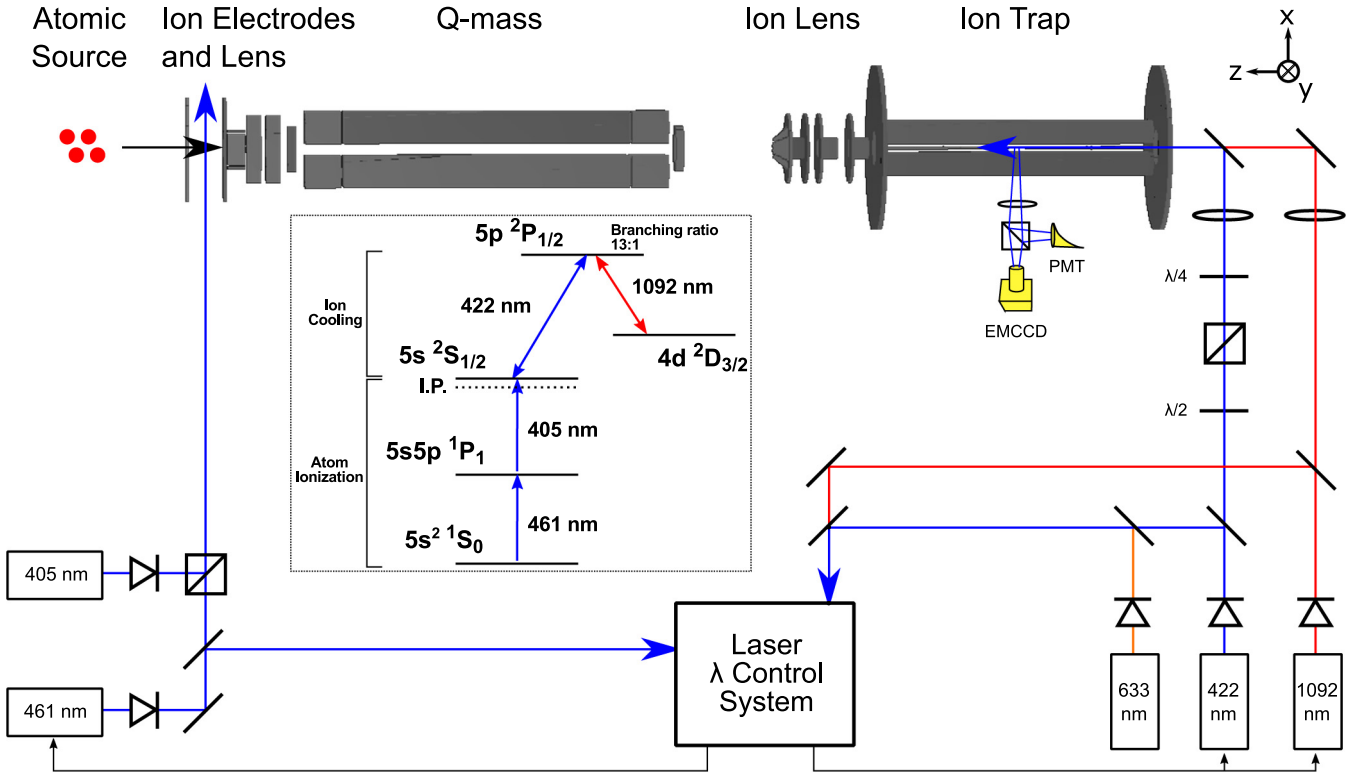

FIG. 1. Schematic diagram of the developed apparatus, the laser arrangement, and the energy levels used for experiments. The diagram of the apparatus is an image rendered by the SIMION program. The 633-nm He-Ne laser is shared for frequency stabilization of the 461-, 422-, and 1092-nm lasers. In order to suppress back-reflected light intensity, a simple isolator combining a $\lambda/2$-wave plate, a polarized beam splitter, and a $\lambda/4$-wave plate was additionally placed in the optical path of the 422-nm laser.

One hundred microliters of the solution were placed on a 0.02-mm-thick titanium foil [13] and dried on a hotplate. Thereafter, the titanium foil was folded and inserted into a carbon crucible. The carbon crucible was set in a furnace, and then the furnace was placed in the chamber. The carbon crucible was resistively heated by passing an electrical current through the water-cooled furnace, resulting in the atomization of the dried solution. The atoms generated from the furnace were ionized by resonance ionization; then they were transported through the metal mesh of a deflector and were guided to a parallel plate. A positive voltage was applied to the deflector electrode on the atomic-vapor-source side, and an extractor electrode on the mass-spectrometer side was grounded in order to extract the ions. The extracted ions were collimated by alignment electrodes and ion lenses.

The mass spectrometer [14] of the mass-analysis section consists of a quadrupole mass filter with a diameter of 0.75 in. and ring-shaped lens electrodes at the entrance and the exit of the filter. Furthermore, pre- and postfilters were attached before and after the mass filter to improve transport efficiency of the ions. The ion beam traveling through the mass spectrometer was expanded in the radial direction, and a number of the ions were lost. Thus, the ion beam was made to converge by a skimmer electrode and a three-stage ion lens, both of which were installed at the rear stage of the mass spectrometer. Because the operation of the mass spectrometer can be computer-controlled through an external port on its main body, we created a mass-spectrometer control program using National Instruments' LABVIEW software. The voltage applied to the ion lenses was determined and optimized with reference to values calculated using the ion-trajectory simulation software SIMION [15].

In the ion-trap section, transported ions were trapped by a linear Paul trap of $r_0 = 6\,\mathrm{mm}$. A laboratory-made power supply capable of generating a sine wave with a trap frequency $\Omega/2\pi = 2.27\,\mathrm{MHz}$ and an rf voltage $V_{\mathrm{rf}} = 50 \sim 750\,\mathrm{V}$ was used to generate the trap potential. The ions were confined along the z axis by eight tapered blades inserted in the trap electrode gap. Four tapered blades were installed on each side of the trap electrodes; the distance between the blade tips on both sides was 11 mm. The symmetrical center of the tapered blades coincides with the center of the trap electrodes. A potential gradient that reduces to a minimum at the trap center was created by applying a uniform positive dc voltage to all the tapered blades. Trapped ions were moved to the center of the trap electrode by this potential gradient.

The laser-induced fluorescence (LIF) emitted by the laser-cooled ions was collected by an observation system located under the trap electrode. In the observation system, the incident light was magnified five times with an objective lens, and only light with a wavelength at 422 nm was selected by a bandpass filter. This light was subsequently split into two beams by a nonpolarizing beam-splitter cube and simultaneously detected by an electron-multiplying CCD (EMCCD) camera and a photomultiplier tube [16].

B. Light sources

The inset in Fig. 1 shows the energy scheme used in this study for the resonance ionization of Sr atoms and the laser cooling of Sr^+ ions. For resonance ionization, we used a two-step ionization scheme of neutral Sr; that is, ground-state atoms were excited via the $5s^2\,{}^1S_0 \rightarrow 5s5p\,{}^1P_1$ transition by a 461-nm laser and then subsequently excited to the $(4d^2 + 5p^2)\,{}^1D_2$ autoionizing state by a 405-nm laser [17]. An external-cavity diode laser (ECDL) with an oscillation wavelength of 461 nm was constructed using an ultraviolet laser diode. For the 405-nm laser, a high-power multimode diode laser was used [18]. The frequency of the 461-nm ECDL was stabilized by a computer-controlled fringe offset lock [19], but that of the 405-nm laser was not. Since the FWHM of the $(4d^2 + 5p^2)\,{}^1D_2$ state is as wide as 1.7 THz [20], stable resonance ionization can be performed without the 405-nm laser stabilization. The frequency of the 461-nm laser was adjusted to the resonance frequency of the isotope with reference to the literature [21].

The ion-cooling scheme is described as follows. For the laser cooling of the Sr^+ ions, the $5s\,{}^2S_{1/2} \rightarrow 5p\ {}^2P_{1/2}$ transition, whose transition rate is as fast as 21.7 MHz [22], was chosen. During the laser cooling, excited ions in the $5p\,{}^2P_{1/2}$ state decay to the $4d\,{}^2D_{3/2}$ metastable state at a ratio of 13:1; then the cooling stops. Therefore, the 1092-nm light is required to close the laser-cooling cycle by repumping the ion to the $5p\,{}^2P_{1/2}$ state. This cooling scheme has been used by various research groups [23–26] since the scheme has a simple structure and the required laser wavelengths are easy to attain. Our group has also succeeded in Sr^+ ion cooling with this cooling scheme [27]. In order to obtain 422- and 1092-nm light, ECDLs were constructed using ultraviolet and infrared laser diodes [28]. The frequencies of both lasers were stabilized by a computer-controlled fringe offset lock [29]. A stabilized HeNe laser was used as a frequency reference of the computer control.

III. RESULTS AND DISCUSSION

A. The $4d\,{}^2D_{3/2} \rightarrow 5p\,{}^2P_{1/2}$ transition isotope shift

The particular resonance frequency information for the $^{90}Sr^+$ ion is required for ion cooling. Although the resonance frequency of the $5s\,{}^2S_{1/2} \rightarrow 5p\ {}^2P_{1/2}$ transition of $^{90}Sr^+$ used in this experiment has not been reported yet, the isotope shift of the $5s\,{}^2S_{1/2} \rightarrow 5p\,{}^2P_{3/2}$ transition has been reported [30,31]. Considering the J dependence of the $5s\,{}^2S_{1/2} \rightarrow 5p\,{}^2P_{3/2}$ transition isotope shift, the $5s\,{}^2S_{1/2} \rightarrow 5p\,{}^2P_{1/2}$ transition isotope shift can be calculated to be $-344(5)$ MHz [32,33]. However, there is no reference for the isotope shift of the $4d\,{}^2D_{3/2} \rightarrow 5p\,{}^2P_{1/2}$ repump transition. Therefore, we evaluated the isotope shift of the $4d\,{}^2D_{3/2} \rightarrow 5p\,{}^2P_{1/2}$ transition of $^{90}Sr^+$ using KING PLOT [34]. The isotope shift $\delta\nu_i^{AA'}$ of transition i between isotopes with mass numbers A and A' can be defined as follows:

$$\delta\nu_i^{AA'} = K_i\left(\frac{M_{A'} - M_A}{M_{A'}M_A}\right) + F_i\delta\langle r_c^2\rangle^{AA'}, \qquad (2)$$

where K is the mass-shift coefficient, F is the field-shift coefficient, M_A is the mass number of the isotope, and $\delta\langle r_c^2\rangle^{AA'}$ is the difference between the mean-square charge radii of the two isotopes. To convert this equation, multiplying both sides of the equation by the factor $M_{A'}M_A/(M_{A'} - M_A)$ results in

$$\frac{M_{A'}M_A}{M_{A'} - M_A}\delta\nu_i^{AA'} = K_i + F_i\frac{M_{A'}M_A}{M_{A'} - M_A}\delta\langle r_c^2\rangle^{AA'}, \qquad (3)$$

where $M_{A'}M_A/(M_{A'} - M_A)\delta\nu_i^{AA'} = \delta\nu_i^{AA'\mathrm{mod}}$ is defined as the modified isotope shift of transition i. If we find the modified isotope shifts for i and j transitions, then we can remove the $\delta\langle r_c^2\rangle^{AA'}$ term, and the following relationship is obtained. From this we can see that the modified isotope shift of the two transitions has a linear relationship.

$$\left(\frac{M_{A'}M_A}{M_{A'} - M_A}\delta\nu_j^{AA'}\right) = \frac{F_j}{F_i}\left(\frac{M_{A'}M_A}{M_{A'} - M_A}\delta\nu_i^{AA'}\right) + K_j - \frac{F_j}{F_i}K_i. \qquad (4)$$

The $^{84}Sr^+$, $^{86}Sr^+$, and $^{88}Sr^+$ isotope-shift values as measured by an ion trap [35] were used to find the linear relationship of their modified isotope shift. For the $5s\,{}^2S_{1/2} \rightarrow 5p\,{}^2P_{1/2}$ transition isotope shift of $^{90}Sr^+$, our calculated value of $-344(5)$ MHz was used. Because the isotope shift of $^{87}Sr^+$ has been investigated only for the $5s\,{}^2S_{1/2} \rightarrow 5p\,{}^2P_{1/2}$ transition and not the $4d\,{}^2D_{3/2} \rightarrow 5p\,{}^2P_{1/2}$ transition [36], its modified isotope shift was not considered in this calculation. As a result, the isotope shift $\Delta\nu^{90-88}$ of the $4d\,{}^2D_{3/2} \rightarrow 5p\,{}^2P_{1/2}$ transition was calculated to be $-302(4)$ MHz. Table I shows all the calculated and referenced isotope-shift values for this calculation.

TABLE I. The $5s\,{}^2S_{1/2} \rightarrow 5p\,{}^2P_{1/2}$ and the $4d\,{}^2D_{3/2} \rightarrow 5p\,{}^2P_{1/2}$ transition isotope shifts of even Sr^+ isotopes. The isotope shifts of $^{84}Sr^+$ and $^{86}Sr^+$ are the reported values of Dubost *et al.* [35]. The $5s\,{}^2S_{1/2} \rightarrow 5p\,{}^2P_{1/2}$ transition isotope shift of $^{90}Sr^+$ is a calculated value. The isotope shift of the $4d\,{}^2D_{3/2} \rightarrow 5p\,{}^2P_{1/2}$ transition of $^{90}Sr^+$ was calculated using KING PLOT.

	$5s\,{}^2S_{1/2} \rightarrow 5p\,{}^2P_{1/2}$ (MHz)	$4d\,{}^2D_{3/2} \rightarrow 5p\,{}^2P_{1/2}$ (MHz)
$\Delta\nu^{84-88}$	−378(4)	+828(4)
$\Delta\nu^{86-88}$	−170(3)	+402(2)
$\Delta\nu^{90-88}$	−344(5)	−302(4)

B. $^{90}Sr^+$ isotope-shift measurement

Because the aim of this research is to confirm the resonance frequency of the radionuclide $^{90}Sr^+$ ion and realize trapping of it, a concentrated solution [37] instead of an environmental sample was used for the convenience of the experiment. The ^{90}Sr isotope abundance of this solution is 8.5×10^{-4}, and the nominal radioactivity is 370 kBq. Since this solution is provided in the form of $SrCl_2$, atomization in this apparatus was able to be carried out by the same reduction process used in Sec. II A. Two titanium foils placed in 200 μL of solution each were used in this experiment because the abundance ratio of the solution is smaller than that of the standard solution.

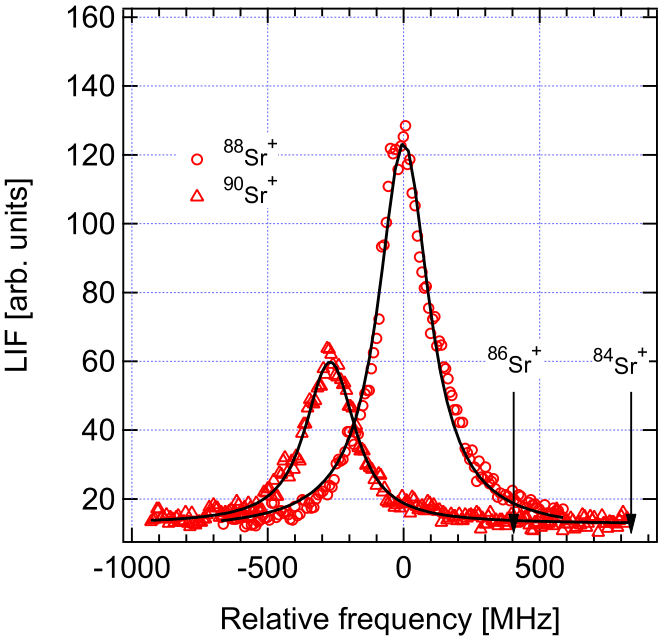

FIG. 2. The $4d\,^2D_{3/2} \rightarrow 5p^2P_{1/2}$ transition spectrum of $^{88}Sr^+$ and $^{90}Sr^+$ ions obtained for the isotope-shift measurement. Each spectrum was acquired three times, and its peak values obtained by Voigt function fitting were averaged. As a result, the isotope shift of $^{88}Sr^+$ and $^{90}Sr^+$ was measured as 281 ± 17 MHz. During 1092-nm laser frequency scanning for the $^{90}Sr^+$ spectrum, LIF of $^{86}Sr^+$ and $^{84}Sr^+$ ions was not observed even if the frequency of the 1092-nm laser was tuned to their resonance frequencies, as shown.

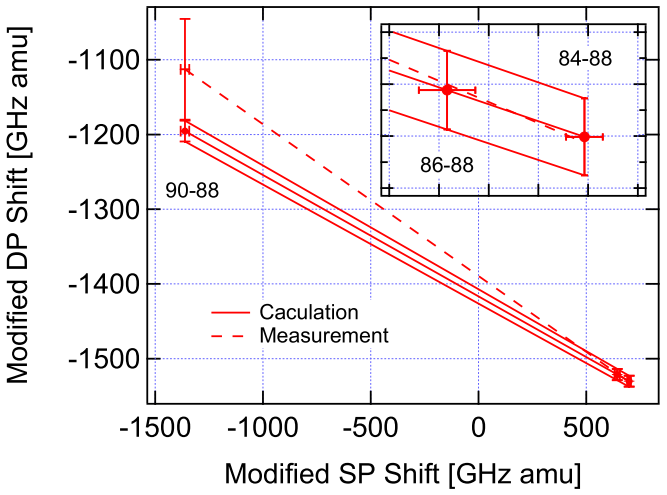

FIG. 3. KING PLOT was used to obtain the $4d\,^2D_{3/2} \rightarrow 5p\,^2P_{1/2}$ transition isotope shift of the $^{90}Sr^+$ ion. From extrapolation of the linear fit obtained by the modified isotope-shift values, the $^{90}Sr^+$ isotope shift was calculated to be $-302(4)$ MHz. To compare this result with the experiment, the modified isotope shift of $\delta\nu_{DP}^{9088mod}$ was calculated using experimentally obtained isotope-shift values and is also shown.

After the ion source was prepared, $^{90}Sr^+$ trap and laser-cooling experiments were conducted. At first, an electrical current of more than 50 A was applied through the furnace to atomize the ^{90}Sr. The frequency of the 461-nm laser was tuned to the resonance of ^{90}Sr, and the 405-nm laser was set in a free-running state for the resonance ionization of atoms. The mass-to-charge ratio of the mass spectrometer was set to 90. For dissipation of the kinetic energy of the transiting ions from the mass-analysis section, helium buffer gas was injected up to a pressure of 1×10^{-4} Torr. The rf voltage applied to the trap electrode for r-direction confinement was 300 V, and a dc voltage of 100 V was applied to the taper blades for z-axis confinement. The frequency of the 422-nm laser was tuned -200 MHz from the resonance of $^{90}Sr^+$ for Doppler cooling, and the laser frequency of the 1092-nm laser was -300 MHz detuned from the resonance of $^{88}Sr^+$. The power of the lasers was 0.7 and 11.8 mW, respectively.

This resulted in the observation of weak ion LIF from the photomultiplier tube. The buffer gas was then evacuated, and the pressure of the ion trap chamber was lowered to 2×10^{-9} Torr to prevent loss of trapped ions due to collision with gas molecules. The rf voltage was reduced from 300 to 200 V in order to mitigate the influence of rf heating [38]. Following this, the 1092-nm laser frequency was swept 1 GHz with respect to the set value to confirm the resonance frequency of the $4d\,^2D_{3/2} \rightarrow 5p\,^2P_{1/2}$ transition. As a result, the LIF reached a maximum at around -280 MHz from the resonance frequency of $^{88}Sr^+$. Resultantly, spectra of $^{90}Sr^+$ and $^{88}Sr^+$ were obtained to confirm accurate values of their isotope shift.

When the $^{90}Sr^+$ spectrum was obtained, all the ions were discarded from the trap; then $^{88}Sr^+$ was loaded into the trap for spectrum capture. Figure 2 shows the spectra of $^{90}Sr^+$ and $^{88}Sr^+$ obtained by this procedure. The x axis of the spectrum was calibrated using the interference fringe signal of an etalon as a frequency marker. The spectrum was taken three times for each isotope. Peaks of the spectra were obtained by fitting with the Voigt function and then averaged. Consequently, the isotope shift $\Delta\nu^{90-88}$ was calculated to be -281 ± 17 MHz. The LIF of $^{86}Sr^+$ and $^{84}Sr^+$ was not observed from the $^{90}Sr^+$ spectrum even when the frequency of the 1092-nm laser was tuned to their resonance frequency. From this result, we can assume that there are no other isotopes except $^{90}Sr^+$ in the trap or only $^{90}Sr^+$ was selectively cooled even if they were present.

This measured value differs by 21 MHz from our calculated value. The reason for this difference can be considered as being due to the particular character of strontium. The atomic nuclear size of strontium reaches its minimum at mass number $A = 88$ and then becomes larger again because the neutron number of ^{88}Sr satisfies the magic number ($N = 50$). Therefore, the modified isotope-shift interval between $\delta\nu_i^{9088mod}$ and $\delta\nu_i^{8688mod}$ is wide. This is easy to understand by comparing the modified isotope-shift values from KING PLOT. The modified isotope shifts obtained from our calculated values and experimental values are shown in Fig. 3. In the calculation result represented by the solid line, the slope of the linear fit was first calculated with respect to $\delta\nu_{SP,DP}^{8688mod}$ and $\delta\nu_{SP,DP}^{8488mod}$. Then the line fit was extrapolated to the modified isotope shift $\delta\nu_{SP}^{9088mod}$ to determine the $4d\,^2D_{3/2} \rightarrow 5p\,^2P_{1/2}$ isotope shift. Further, the modified isotope shift of the measured value -281 ± 17 MHz is also shown in Fig. 3. The values $\delta\nu_{SP,DP}^{8688mod}$ and $\delta\nu_{SP,DP}^{8488mod}$ are connected by the dashed line. Straight lines traced by both the calculated value and the experimental value are within the error range. For a detailed confirmation, an inset of the expanded

area for $\delta\nu_{\mathrm{SP,DP}}^{8688\mathrm{mod}}$ and $\delta\nu_{\mathrm{SP,DP}}^{8488\mathrm{mod}}$ is shown in the top right of Fig. 3. However, a deviation occurs at $\delta\nu_{\mathrm{DP}}^{9088\mathrm{mod}}$ between the calculated value and the measured value in the process of extrapolating the value to a large range since $\delta\nu_{\mathrm{SP}}^{9088\mathrm{mod}}$ is far away from $\delta\nu_{\mathrm{SP}}^{8688\mathrm{mod}}$. It is reasonable to think that this deviation is caused by taking a large extrapolation rather than the uncertainty of the $\Delta\nu^{84-88}$ and $\Delta\nu^{86-88}$ isotope shifts. But since the FWHM of the $4d\,^2D_{3/2} \rightarrow 5p\,^2P_{1/2}$ transition is as wide as a few hundred megahertz, repumping took place, and ion LIF could be obtained even if the frequency of the 1092-nm laser was detuned by a few tens of megahertz from its resonance during ion loading. After that, the $^{90}Sr^+$ resonance frequency of the $4d\,^2D_{3/2} \rightarrow 5p\,^2P_{1/2}$ transition could be measured systematically by sweeping the frequency of the 1092-nm laser.

C. Individual ion imaging

Individual trapped ions can be observed when the temperature of laser-cooled ions is sufficiently decreased to result in crystallization. The observation of such makes it possible to eliminate the effects of isobaric and background signals from the LIF signal by direct counting of the ion image. We conducted an experiment to find whether trapped clouds ions can be crystallized into individual ions by laser cooling in our apparatus, achieving a background-free observation of $^{90}Sr^+$.

The procedure for loading ions into the trap is the same as described in Sec. III C. However, this time the frequency of the 1092-nm laser was tuned to −280 MHz, which is the resonance frequency of $^{90}Sr^+$ confirmed by this research, rather than setting it to the calculated value of −300 MHz. When the ion LIF was confirmed, the buffer gas was exhausted, and the rf voltage was reduced. After that, we successfully crystallized the ions by bringing the frequency of the 422-nm laser close to its resonance frequency. Figure 4(a) shows the trapped ion image obtained by the EMCCD camera after loading. The frequency of the 422-nm laser is −200 MHz detuned from its resonance. Trapped ions are kept in the cloud phase because the laser-cooling efficiency could not be increased for the experimental conditions. When the loaded $^{90}Sr^+$ LIF was confirmed, the buffer gas was exhausted from 1×10^{-4} to 2.2×10^{-9} Torr over a few minutes. The rf voltage was reduced from 300 to 200 V, and the number of trapped ions was reduced to suppress the rf heating. The frequency of the 422-nm laser was tuned from −200 to −40 MHz relative to the resonance frequency. Consequently, four sufficiently laser-cooled $^{90}Sr^+$ ions were crystallized and observed, as shown in Fig. 4(b). The calculated ion interval was 26 μm considering the magnification of the observation system. There is no report on trapping the radioactive isotope $^{90}Sr^+$ with ion traps and observing the individual ions as far as we know. Based on the above results, it was confirmed that a $^{90}Sr^+$ background-free observation is possible with our developed apparatus.

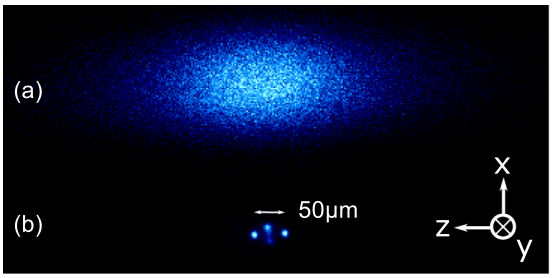

FIG. 4. Trapped $^{90}Sr^+$ ion image captured by the EMCCD camera. One second of exposure time and 5× magnification were applied for the image. The coordinates and the scale are the same for both (a) and (b). In (a), the ions are in a cloud phase since the laser cooling had not yet been sufficiently performed. However, four crystallized $^{90}Sr^+$ ions were observed by efficient cooling in (b). The gap between ions was measured to be 26 μm.

IV. CONCLUSIONS

We have developed an apparatus combining resonance ionization and an ion-trap technique. Sr^+ isotope ions were generated by resonance ionization, and trapped ions were laser cooled in the apparatus. The $4d\,^2D_{3/2} \rightarrow 5p\,^2P_{1/2}$ transition isotope shift of $^{90}Sr^+$ was calculated using KING PLOT. For verification of this result by experiment, $^{88}Sr^+$ and $^{90}Sr^+$ ions were individually trapped in the apparatus, and their spectra were acquired. As a result, we succeeded in trapping $^{90}Sr^+$ ions and found that there was a 21-MHz deviation between our calculated value and the experimentally measured value. The modified isotope shift $\delta\nu_{\mathrm{DP}}^{9088\mathrm{mod}}$ deviated from other isotope-shift values because of an extrapolation error due to the characteristics of the strontium nucleus. However, we were able to measure an experimental value as described by this research. In addition, $^{90}Sr^+$ laser cooling was performed using the resonance frequency value confirmed by the experiment. Consequently, the trapped ions were laser cooled, and the crystallized $^{90}Sr^+$ individual ions were successfully observed from the EMCCD camera. From these results, it was confirmed that background-free observation of $^{90}Sr^+$ is possible with our apparatus.

ACKNOWLEDGMENTS

Part of this study was the result of "Development of rapid analysis method of ^{90}Sr in marine products using lasers" carried out under the Strategic Promotion Program for Basic Nuclear Research by the Ministry of Education, Culture, Sport, Science and Technology of Japan (MEXT). Also, this work was supported by JSPS KAKENHI Grant No. JP16H04639. The authors appreciate valuable discussion with Prof. K. Wendt of the University of Mainz and are thankful for technical assistance from the radiation control and technical divisions of the Tokai Campus of The University of Tokyo.

[1] S. K. Sahoo, N. Kavasi, A. Sorimachi, H. Arae, S. Tokonami, J. W. Mietelski, E. Okas, and S. Yoshida, Sci. Rep. **6**, 23925 (2016).

[2] N. Vajda and C.-K. Kim, Appl. Radiat. Isot. **68**, 2306 (2010).

[3] Y. Takagai, M. Furukawa, Y. Kameo, and K. Suzuki, Anal. Methods **6**, 355 (2014).

[4] B. A. Bushaw and B. D. Cannon, Spectrochim. Acta, Part B **52**, 1839 (1997).
[5] J. Eschner, G. Morigi, F. Schmidt-Kaler, and R. Blatt, J. Opt. Soc. Am. B **20**, 1003 (2003).
[6] J. I. Cirac and P. Zoller, Phys. Rev. Lett. **74**, 4091 (1995).
[7] G. P. Barwood, G. Huang, H. A. Klein, L. A. M. Johnson, S. A. King, H. S. Margolis, K. Szymaniec, and P. Gill, Phys. Rev. A **89**, 050501(R) (2014).
[8] R. C. Thompson, Meas. Sci. Technol. **1**, 93 (1990).
[9] Y. Hashimoto, D. Nagamoto, and S. Hasegawa, Int. J. Mass Spectrom. **279**, 163 (2009).
[10] M. Kitaoka, K. Jung, Y. Yamamoto, T. Yoshida, and S. Hasegawa, J. Anal. At. Spectrom. **28**, 1648 (2013).
[11] Y. Yamamoto and S. Hasegawa, IEEJ Trans. Electr. Electron. Eng. **8**, 599 (2013).
[12] The Sr standard solution was from Hayashi Pure Chemical, I2-13-2.
[13] Titanium foil was from Niraco, TI-453212.
[14] The mass spectrometer used was Extrel, 2.1-MHz 150-QC.
[15] D. A. Dahl, Int. J. Mass Spectrom.**200**, 3 (2000).
[16] The objective lens was a Nikon, CM-5A 5xA. The bandpass filter was an Edmund, 34-497, and the nonpolarizing beam-splitter cube was also from Edmund, 49-682. The EMCCD camera was from Andor, iXon 888, and the photomultiplier tube was a Hamamatsu H10682-210.
[17] M. Brownnutt, V. Letchumanan, G. Wilpers, R. C. Thompson, P. Gill, and A. G. Sinclair, Appl. Phys. B **87**, 411 (2007).
[18] The ultraviolet laser diode was from Nichia, NDB 4311T, with a center wavelength of 461 nm. The high-power multimode diode laser was from CNI Laser, MD-405-HS-1W.
[19] M. Miyabe, M. Oba, M. Kato, I. Wakaida, and K. Watanabe, J. Nucl. Sci. Technol. **43**, 305 (2006).
[20] W. Mende, K. Bartschat, and M. Kock, J. Phys. B **28**, 2385 (1995).
[21] B. A. Bushaw and W. Nörtershäuser, Spectrochim. Acta, Part B **55**, 1679 (2000).
[22] A. Gallagher, Phys. Rev. **157**, 24 (1967).
[23] A. G. Sinclair, M. A. Wilson, and P. Gill, Opt. Commun. **190**, 193 (2001).
[24] D. J. Berkeland, Rev. Sci. Instrum. **73**, 2856 (2002).
[25] S. Removille, R. Dubessy, B. Dubost, Q. Glorieux, T. Coudreau, S. Guibal, J.-P. Likforman, and L. Guidoni, J. Phys. B **42**, 154014 (2009).
[26] A. A. Madej, P. Dube, Z. Zhou, J. E. Bernard, and M. Gertsvolf, Phys. Rev. Lett. **109**, 203002 (2012).
[27] K. Jung, K. Yamamoto, Y. Yamamoto, M. Miyabe, I. Wakaida, and S. Hasegawa, Jpn. J. Appl. Phys. **56**, 062401 (2017).
[28] For the laser diodes the ultraviolet one was from Nichia, NDV4A16E, with a center wavelength of 422 nm, and the infrared one was from Toptica, LD-1080-0300-1, with a center wavelength of 1092 nm. The stabilized HeNe laser was a Thorlabs, HRS015, 633 nm.
[29] K. Jung, Y. Yamamoto, and S. Hasegawa, Hyperfine Interact. **236**, 39 (2015).
[30] R. E. Silverans, P. Lievens, L. Vermeeren, E. Arnold, W. Neu, R. Neugart, K. Wendt, F. Buchinger, E. B. Ramsay, and G. Ulm, Phys. Rev. Lett. **60**, 2607 (1988).
[31] F. Buchinger, E. B. Ramsay, E. Arnold, W. Neu, R. Neugart, K. Wendt, R. E. Silverans, P. Lievens, L. Vermeeren, and D. Berdichevsky, Phys. Rev. C **41**, 2883 (1990).
[32] K. Wendt, S. A. Ahmad, F. Buchinger, A. C. Mueller, R. Neugart, and E.-W. Otten, Z. Phys. A **318**, 125 (1984).
[33] K. Wendt (Private communication).
[34] W. H. King, *Isotope Shifts in Atomic Spectra* (Springer, New York, 1984).
[35] B. Dubost, R. Dubessy, B. Szymanski, S. Guibal, J.-P. Likforman, and L. Guidoni, Phys. Rev. A **89**, 032504 (2014).
[36] G. Borghs, P. D. Bisschop, M. V. Hove, and R. E. Silverans, Hyperfine Interact. **15**, 177 (1983).
[37] The concentrated solution was from Japan Radioisotope Association, SR005, 3 mL.
[38] R. Blumel, C. Kappler, W. Quint, and H. Walther, Phys. Rev. A **40**, 808 (1989).